Clim. Past Discuss., 9, 583–613, 2013
www.clim-past-discuss.net/9/583/2013/
doi:10.5194/cpd-9-583-2013

Climate of the Past Discussions

Cyclone trends constrain monsoon variability during Late Oligocene sea level highstands (Kachchh Basin, NW India)

M. Reuter[1], **W. E. Piller**[1], **M. Harzhauser**[2], **and A. Kroh**[2]

[1]Institute for Earth Sciences, University of Graz, Heinrichstraße 26, 8010, Graz, Austria
[2]Department of Geology and Palaeontology, Natural History Museum Vienna, Burgring 7, 1010 Vienna, Austria

Received: 13 December 2012 – Accepted: 9 January 2013 – Published: 24 January 2013

Correspondence to: M. Reuter (markus.reuter@uni-graz.at)

Published by Copernicus Publications on behalf of the European Geosciences Union.

Abstract

Important concerns about the consequences of climate change for India are the potential impact on tropical cyclones and the monsoon. Herein we present a sequence of fossil shell beds from the shallow-marine Maniyara Fort Formation (Kachcch Basin) as an indicator of tropical cyclone activity along the NW Indian coast during the Late Oligocene warming period (~ 27–24 Ma). Direct proxies providing information about the atmospheric circulation dynamics over the Indian subcontinent at this time are important since it corresponds to a major climate reorganization in Asia that ends up with the establishment of the modern Asian monsoon system in the Early Miocene. The vast shell concentrations comprise a mixture of parautochthonous and allochthonous assemblages indicating storm-generated sediment transport from deep to shallow water during third-order sea level highstands. Three distinct skeletal assemblages were distinguished each recording a relative storm wave base depth. (1) A shallow storm wave base is shown by nearshore mollusks, corals and *Clypeaster* echinoids; (2) an intermediate storm wave base depth is indicated by lepidocyclind foraminifers, *Eupatagus* echinoids and corallinaceans; and (3) a deep storm wave base is represented by an *Amussiopecten–Schizaster* echinoid assemblage. Vertical changes in these skeletal associations give evidence of gradually increasing tropical cyclone intensity in line with third-order sea level rise. The intensity of cyclones over the Arabian Sea is primarily linked to the strength of the Indian monsoon. Therefore and since the topographic boundary conditions for the Indian monsoon already existed in the Late Oligocene, the longer-term cyclone trends were interpreted to reflect monsoon variability during the initiation of the Asian monsoon system. Our results imply an active monsoon over the Eastern Tethys at ~ 26 Ma followed by a period of monsoon weakening during the peak of the Late Oligocene global warming (~ 24 Ma).

CPD
9, 583–613, 2013

Cyclone trends constrain monsoon variability

M. Reuter et al.

1 Introduction

Cyclones are one of the most devastating natural hazards that affect tropical coasts (Henderson-Sellers et al., 1998). For this reason, attempts to associate tropical cyclone trends with global change have become a challenging subject in recent years (e.g. Goldenberg et al., 2001; Webster et al., 2005; Klotzbach, 2006; Holland and Webster, 2007; Elsner et al., 2008; Emanuel et al., 2008; Vecchi and Knutson, 2008; Evan et al., 2011). Although future predictions consistently indicate that greenhouse warming will cause the globally averaged intensity of tropical cyclones to shift towards stronger storms (Solomon et al., 2007), the limited instrumental record and deficient availability and quality of global historical records impede extensive analyses of the natural cyclone variability in most of the tropical cyclone basins (Henderson-Sellers et al., 1998). Therefore, it remains uncertain whether current changes in tropical cyclone activity have exceeded the variability expected from natural causes (Knutson et al., 2010). The Indian Ocean including the Arabian Sea and the Bay of Bengal are of particular concern because of the high population density along their coastlines (Charabi, 2010). In the Arabian Sea most storms tend to be small and dissipate quickly (Charabi, 2010). However, the wind circulation pattern over the northern Arabian Sea has changed over the last 30 yr allowing stronger storm development (Evan et al., 2011). As a result, the Saurashtra and Kachchh regions at the northwestern coast of India have been increasingly subject to severe cyclonic storms in recent years (Nigam and Chaturvedi, 2006). This change of atmospheric circulation is, however, considered to occur independently from global warming and interpreted to be related to the increasing anthropogenic buildup of aerosols in the atmosphere over India and the Indian Ocean leading to a weakening of the vertical wind shear over the Arabian Sea (Evan et al., 2011).

In the geological record storm events could have been preserved as tempestite beds and temporal variations in their abundance and thickness provide information about palaeostorm intensities and frequencies (Brandt and Elias, 1989; Long, 2007). Herein we present a shallow-marine tempestite sequence from the Maniyara Fort Formation

CPD
9, 583–613, 2013

in the Kachchh Basin (Gujarat, NW India) as a record for natural cyclone activity during the Late Oligocene. This time is of peculiar importance for the Asian climate evolution because the climate pattern changed from zonal to monsoon-dominant at the Oligocene–Miocene transition (Guo et al., 2008). The timing of this important climate shift and the behavior of the atmospheric circulation pattern over Asia during its early stages remained, however, poorly constrained since well-dated direct climate proxies are scarce (Dupont-Nivet et al., 2008; Quan et al., 2011).

2 Geological setting and locality

The Kachchh Basin is a peri-cratonic rift basin at the western passive continental margin of India (Biswas, 2005) (Fig. 1). It opened since the Late Triassic–Early Jurassic due to the break-up of the Gondwana supercontinent and the subsequent counter-clockwise north-drift of the separated Indian subcontinent (Biswas, 1982, 1987; Ali and Aitchison, 2008). A 3000-m-thick succession of predominantly siliciclastic shallow-marine and fluvio-deltaic sediments was deposited during the synrift stage (Biswas, 1982, 1992, 2005). The rifting ceased in the Late Cretaceous due to the beginning collision of India and Asia. After a phase of effusive Deccan Trap volcanism (Biswas and Deshpande, 1973; Saunders et al., 2007), uplift occurred along the entire western Indian rifted margin during the Eocene–Oligocene (Shanker, 2001). It was initiated by the commencement of subduction of oceanic crust below the Tibetan Plate, which stopped the free-drift of the subcontinent (Shanker, 2001). The resultant compressive stress regime caused the uplift and tilting of tectonic blocks in the Kachchh Basin (Biswas, 2005). The largest one was the SW-tilted Kachchh Mainland Uplift (KMU), which extends over 150 km in northwest–southeast direction (Fig. 1).

The studied outcrop is located along the bed of the Bermoti River in the surrounding of the village Bermoti (N 23° 27′ 45″, E 68° 36′07″, Fig. 1) and represents the type locality of the Oligocene Maniyara Fort Formation (Biswas and Raju, 1971; Biswas, 1992). The exposed sedimentary succession was deposited in marginal marine, littoral to shallow inner-shelf environments on the $< 10^{\circ}$ inclined homoclinal dip-slope ramp of the KMU (Biswas, 1992; Harzhauser et al., 2009). Following Biswas (1992), the Maniyara Fort Formation includes four informal lithostratigraphic members: (1) the Basal Member, (2) the Lumpy Clay Member, (3) the Coral Limestone Member, and (4) the Bermoti Member. The Basal Member comprises alternating beds of foraminiferal limestone, glauconitic siltstone and calcareous, gypsiferous claystone. The Lumpy Clay Member includes calcareous, lumpy claystones with thin intercalated limestone and marl beds. The Coral Limestone Member is defined as a succession of biosparites and glauconitic biomicrites. Calcareous claystones are intercalated in its lower part, while its upper part is characterized by small coral bioherms. The transition to the Bermoti Member is marked by the sudden appearance of glauconite in ochre coloured sandstones with abundant vertebrate remains. The carbonatic Maniyara Fort Formation is overlain by siliciclastics of the Khari Nadi Formation of Aquitanian age (Biswas, 1992). The siliciclastic sedimentation prevailed until present-day (Biswas, 1992).

3 Methods

Bermoti river section was measured bed-for-bed The primary dataset consists of sedimentological information gathered through field observations and 50 thin-sections (5 × 5 cm). Sedimentological data include lithology, sedimentary texture, sedimentary structures, nature of bedding and bedding contacts, fossil content, and lateral variability. Due to their large size, the abundances of the major components in the shell beds have been estimated semi-quantitatively in the field.

4 Results

The measured section has a total thickness of about 31 m and represents the upper part of the Coral Limestone Member (6 m) and the Bermoti Member (12 m) of the

CPD
9, 583–613, 2013

carbonatic Maniyara Fort Formation as well as the lower part of the siliciclastic Khari Nadi Formation (13 m, Fig. 2).

4.1 Maniyara Fort Formation

Generally, the Maniyara Fort Formation is characterized by a partly dolomitic succession of bioturbated wackestones, packstones and marls alternating with massive matrix-rich skeletal rudstones of 0.2 to 0.8 m thickness (Fig. 2). Typically the skeletal rudstones are poorly sorted and dominated by variable amounts of larger benthic foraminifers molluscs echinoids, bryozoans and corallinaceans in a bioclastic packstone matrix. The skeletal components are mostly fragmented and randomly orientated. Bivalve shells are always disarticulated. Usually, the coarse-grained carbonates form vast sheets, which can be exposed over some 100 m^2 in the outcrop without showing a difference in thickness or facies. The contact to the underlying sediments is always sharp.

4.1.1 Coral Limestone Member

In the lower part of the Coral Limestone Member the skeletal rudstone sheets are mainly formed by lepidocyclinids up to 2 cm in diameter and biconvex discoidal in shape. Nummulitids, gastropods (e.g. *Ampullinopsis crassatina*), pectinids (*Aequipecten*), coral fragments (*Acropora*) and echinoids (*Clypeaster*, *Eupatagus*) are associated (Fig. 2). Five species of Nummulitidae (*Nummulites* aff. *vascus*, *N. fichteli*, *N. sublaevigatus*, *Operculina complanata*) and one of Lepidocyclinidae (*Eulepidina dilatata*) were identified in the larger foraminiferan rudstones of the Coral Limestone Member. The upper surface of the larger foraminiferan concentrations can be encrusted by several decimetre high coral heads or colonized by in situ tubes of the teredinid bivalve *Kuphus* (Fig. 2). Large, horizontal burrow systems of decapods can also occur at the top of larger foraminiferan deposits. The uppermost lepidocyclinid limestone bed in the Coral Limestone Member was deposited above a ferruginous crust and is

CPD
9, 583–613, 2013
Cyclone trends constrain monsoon variability
M. Reuter et al.

characterized by abundant corallinaceans and detritic glauconite in a muddy dolomitic matrix. In contrast to all other sheet-like shell beds in Maniyara Fort Formation, this bed has a wedge-shaped profile, which is decreasing in thickness from 1 m in the NE to 0.25 m in the SW over a distance of 60 m (Fig. 2).

The upper part of the Coral Limestone Member is characterized by small patch reefs (Fig. 2). They are interfingering with fine-grained fossiliferous platy limestones that contain bivalves (*Aequipecten*, *Cyathula*, *Lucinoma*, cardiids, tellinids), solitary corals and abundant ostracods (*Bairdia*). Notably, the surface of the patch reef at the top of the Coral Limestone Member is intensively bored by bivalves and encrusted by corallinaceans. This patch reef is also surrounded by a skeletal rudstone composed of bivalves (cardiids, tellinids, *Lucinoma*, *Cyathula*, *Aequipecten*) gastropods, irregular echinoids (*Echinocyamus bernaniensis*: abundant, *Eupatagus*: rare), coral clasts as well as rare larger benthic foraminiferan tests (*Nummulites*, lepidocyclinids) of small size.

4.1.2 Bermoti Member

The Bermoti Member starts with a yellow, 1.25-m-thick dolomite with detritic glauconite and ferriclastic sand content (Fig. 2) It is overlain by a 40 cm thick, dolomitic sandy (ferriclast sand) rudstone with gastropods (e.g. *Ampullinopsis crassatina*, *Campanile pseudoobeliscus*, *Cerithium bermotiense*, *Dilatilabrum sublatissimum*, *Persististrombus radix*, *Lyria (Indolyria) maniyaraensis*; see Harzhauser et al., 2009 for the full list), bivalves (*Aequipecten, Cyathula*), echinoids (*Clypeaster sowerbyi*: abundant, *Eupatagus singhi*: rare, *Prionocidaris*: common), coral clasts, small *Nummulites* (rare), bryozoans and vertebrate bones. Remarkable is the abundant occurrence of articulated crabs (*Palaeocarpilius rugifer*, *Neptunus wynneanus*) and of rare nautilids. The upper surface of this bed is covered by a thin ferruginous crust (Fig. 2). Above follows a 2-m-thick unit of well-sorted, brown ferriclastic sandstone with a 15-cm-thick shell bed in the upper part. It is dominated by a gastropod fauna, which is similar to that of the previous shell bed (Harzhauser et al., 2009). Echinoids (*Clypeaster*, cidaroids) pectinid bivalves (*Aequipecten*, *Amussiopecten*) as well as lepidocyclinids and vertebrate bones are further characteristic biotic constituents. The sandstones are overlain by a 90-cm-thick dolomitic wackestone with mass-occurring *Bairdia* ostracods and in situ *Kuphus* tubes at the top. It is covered by a 2-m-thick wackestone-skeletal rudstone alternation (Fig. 2). *Amussiopecten* and irregular echinoids (*Schizaster sufflatus*) dominate the skeletal assemblages in the rudstones. Lepidocyclinids, gastropods and *Eupatagus* echinoids are associated. The gastropod faunas are similar to that at the base of the Bermoti Member. *Eupatagus* can be very frequent in lepidocyclinid-rich deposits. *Callianassa* burrows at the contact to the underlying wackestones are filled with coarse skeletal debris. In situ tubes of *Kuphus* can occur at the top of rudstone beds. In the upper part the Bermoti Member shows again dolomitization (Fig. 2). The skeletal assemblages of the rudstone sheets in this part of the section are dominated by biconvex discoidal lepidocyclinids (*Eulepidina dilatata*; 2 cm Ø) and corallinacean branches. A thin (5 cm) bed of poorly sorted, bioclastic lithoclast rudstone is intercalated in the upper part of this unit. It is well-winnowed and dominated by angular lepidocyclinid limestone lithoclasts < 1.5 cm. Dolomite clasts, ferricrete clasts and quartz grains are present as well. The top of the Bermoti Member is represented by a red mottled dolomite with ferriclastic sand (Fig. 2).

4.2 Khari Nadi formation

The Khari Nadi Formation starts with a 5-m-thick, brown pebbly-cobbly, grain-supported conglomerate composed of well-rounded and polished ferricrete grains and single pebbles of white agate (Fig. 2). The conglomerate exhibits clinoforms dipping 19° to the SW. Upsection and towards the SW it passes into fine-grained siliciclastic sediments (sandy silts, silty clays, fine-grained sandstones).

CPD
9, 583–613, 2013

5 Discussion

5.1 Depositional environments

For the Maniyara Fort Formation a mainly shallow restricted inner ramp environment is indicated by the occurrence of in situ *Kuphus* tubes (Reuter et al., 2008) an individual-rich, monotypic (*Bairdia*) ostracod assemblage in the micrite-rich facies (Kornicker, 1961) and common dolomitization (Fig. 2). The formation of dolomite is considered to be an early diagenetic process because it is restricted to distinct beds and within close stratigraphic proximity to emergence horizons. Pedogenesis during partial emergence of the KMU and denudation of lateritic soils that formed on exposed Deccan Trap basalts during the Eocene (Valeton, 1999) are documented by ferruginous crusts and red motteling as well as intercalations of ferriclastic sand at the base and top of the Bermoti Member (Fig. 2).

The presence of in situ coral patch reefs and the highly diverse nearshore marine gastropod faunas (Harzhauser et al., 2009) indicate less restricted shallow marine environments. Giant conchs such as *Dilatilabrum sublatissimus* are found today in seagrass meadows and sheltered lagoons, where they live partly buried in the soft substrate (Bandel and Wedler, 1987). Extant *Clypeaster* echinoids also occur most commonly in sandy sediments with seagrass patches (Hendler et al., 1995).

The occurrences of glauconite grains, however, contradict an episodically emerged shallow ramp setting since this mineral is commonly considered to form at outer-shelf or even greater depths (> 100 m; El Albani et al., 2005). Because the glauconitic deposits are associated with ferruginous crusts and ferriclastic sand (Fig. 2), it is, however, more likely that the detritic glauconite derived from the reworking of the glauconite-bearing sediments from the Basal Member of the Maniyara Fort Formation. Nonetheless, the biotic assemblages in the skeletal rudstone facies contain substantial amounts of deeper water indicators, which are completely lacking in the micrite-rich limestone and reef facies (Fig. 2) suggesting extensive sediment transport from deep to shallow water. Consistently with this interpretation, the overall high degree of fragmentation and

CPD
9, 583–613, 2013

disarticulation in the shell beds indicate sediment transport. Larger benthic foraminifers were apparently susceptible to resedimentation as they lack any form of attachment or stabilization after death (Pedley, 1998). Following the idealized ramp profile of Pedley (1998) for the central Mediterranean Oligocene–Miocene ramps, autochthonous larger benthic foraminiferan facies with coralline algae extend from the only few meters deep coral patch reef zone towards deeper middle ramp settings. Thereby, the size of the same lepidocyclinid species increases with greater water depth and their shape changes from very inflated to flat. Flat discoidal *Lepidocyclina* tests with diameters > 3 cm represent the greatest water depth in this model (~ 40–60 m). The smaller size and more biconvex shape of the lepidocyclinids in the Maniyara Fort Formation indicate a shallower palaeodepth at their living place. Accordingly, palaeoenvironmental models show that large perforate hyaline benthic foraminifers such as *Lepidocyclina*, *Nummulites* and *Operculina complanata* thrived in the lower part of the upper photic zone (Bassi et al., 2007).

In Bermoti River section *Eupatagus* is most common in lepidocyclinid concentrations (Fig. 2). Live *Eupatagus* is commonly found between 10 m and 60 m water depth on coral sands of the fore reef slope (Mortenson, 1951; de Ridder, 1984; Schultz, 2005, 2009). Although little is known about its ecology, a functional morphological approach suggests that it is shallow burrowing (Kanazawa, 1992). Morphologically similar forms with enlarged spines are capable of rapid re-burial after disturbance, which allows settlement of higher-energy habitats disturbed by wave turbulence.

The skeletal assemblages of the shell beds in the middle part of the Bermoti Member are dominated by *Amussiopecten* and irregular echinoids (*Schizaster sufflatus*), which both do not occur in the interbedded micrite-rich facies (Fig. 2). The extinct genus *Amussiopecten* is morphologically very close to the extant *Amusium* with its type species *Amusium pleuronectes.* Both are characterised by light and disc-shaped shells often with moderate ribbing. Modern *Amusium* preferentially live in few tens of meters water depth. *Amusium pleuronectes* is most common between 18–40 m water depth (Brand, 2006) and *Amusium balloti* is typically found in 30–60 m water depth

CPD
9, 583–613, 2013

(Himmelman et al., 2009). Accordingly, comparable pectinid shell beds in the Burdigalian of Egypt, characterised by low diversity, thin shells and weak sculpturing, were interpreted to have formed by winnowing in few tens of meters water depth (20–40 m) close to the storm wave base (Mandic and Piller, 2001). Although *Schizaster* echinoids are reported from more than 350 m water depth, most *Schizaster* species occur in inner neritic environments (5–100 m) at present-day (Mortensen, 1951). The distribution of *Schizaster* seems controlled by the availability of suitable soft sediment bottoms. There *Schizaster* clearly prefers habitats with muddy silt to fine sand substrates, exploiting bacterial and meiofaunal food sources accumulated at the redox discontinuity potential layer (Schinner, 1993). Due to this habitat preference *Schizaster* is usually found in protected shallow or deeper settings where a sufficiently thick layer of fine-grained sediment is present. Since *Schizaster sufflatus* is always associated with *Amussiopecten* in the Maniyara Fort Formation a deeper habitat is indicated.

Bioclast-filled *Callianassa* burrows below the erosive base of a shell bed as well as a larger foraminiferan limestone breccia give evidence for high-energetic event deposition (Wanless et al., 1988; Seilacher and Aigner, 1991). Rapid burial during a catastrophic sedimentation event might also be responsible for the in situ preservation of articulated crabs in the shell bed at the base of the ferriclastic unit (Brett and Seilacher, 1991). The random orientation of skeletal elements in the poorly sorted shell beds as well as the occurrence of in situ *Kuphus* tubes and large decapod burrows at their top reveal a biological overprint that obliterated primary bedding features (Sepkowski et al., 1991). Notably, the surface of the coral patch reef at the top of the Coral Limestone Member, which is flanked by a skeletal rudstone (Fig. 2) is intensively bored by bivalves and encrusted by corallinaceans. This suggests that bioclastic event sedimentation had suffocated the corals at first and later the unconsolidated bioclastic sediment was removed by agitated water from the highest elevated part of the buildup so that dead coral surfaces became exposed and subject to intense bivalve boring and biogenic encrustation.

CPD
9, 583–613, 2013

The ferriclastic conglomerate at the base of the Khari Nadi Formation (Fig. 2) shows the foreset/topset-pattern of a SW prograding Gilbert-type delta. Associated pebbles of white agate indicate that the ferriclasts originate from the erosion of lateritic crusts that developed on weathered Deccan Trap basalts.

5.2 Biostratigraphy and sequence stratigraphic correlation

Biswas (1992) assumed a Rupelian age for the Coral Limestone Member based on the presence of *Eulepidina dilatata* and *Nummulites fichteli* and a Chattian age for the Bermoti Member due to its typical fauna. In fact, the presence of *N. fichteli*, *N.* aff. *vascus*, *N. sublaevigatus* and *E. dilatata* indicates an early Chattian age (SBZ22b of Cahuzac and Poignant, 1997) for the lower part of the Coral Limestone Member, while the absence of *Nummulites* and the presence of *E. dilatata* suggest a late Chattian age (SBZ23 of Cahuzac and Poignant, 1997) for the upper part of the Bermoti Member (Fig. 3).

Due to its position in the inner Kachchh Basin (Fig. 1) the KMU was isolated from coarse-grained terrigenous discharge which may have entered the basin from the continent. Only clay minerals had the chance to arrive on the carbonate ramp as suspension load from the basin margins. Therefore coarse-grained terrigenous fraction must have local sources in the area of the KMU during relative sea level lowstands. The studied sedimentary record includes three relative sea level lowstands in the early Chattian–Aquitanian time interval. These correlate with three sea level lowstands of third-order in the sequence-chronostratigraphic chart of Hardenbol et al. (1998) (Fig. 3). The recognition of the Chattian/Aquitanian boundary at the contact between the Maniyara Fort Formation and the Khari Nadi Formation (Biswas, 1992) assigns this surface to the lowstand that produced the Ch4/Aq1 sequence boundary (Fig. 3) of Hardenbol et al. (1998). The penultimate relative sea level lowstand, which is documented by the ferriclastic sandstones in the lower part of the Bermoti Member (Fig. 2), correlates then with the sea level lowstand that produced the Ch3 sequence boundary of Hardenbol et al. (1998). The first relative sea level lowstand is represented by the deposition of reworked glauconite above a ferruginous crust in the Coral Limestone Member (Fig. 2). Since it is dated to the shallow benthic foraminifera zone SBZ22b it is correlated with the sea level lowstand that produced the Ch2 sequence boundary of Hardenbol et al. (1998).

5.3 Effects of sea level and tectonic uplift on sedimentation

The constantly very shallow depositional environments throughout the Maniyara Fort Formation show that even few meters sea level fall must have caused the emergence of the KMU ramp at the Bermoti River locality. Since the amplitudes of the Late Oligocene third-order sea level cycles were in the range of several tens of meters (Hardenbol et al., 1998) the study site could have been inundated therefore only during their highstands (Fig. 3). Dolomitization as well as reworking and input of terrigenous sediment characterize the early and late highstands while more open marine conditions enabled coral reef growth during maximum flooding (Fig. 3). The increasing restriction of the KMU carbonate ramp during the Oligocene, which is displayed by the increasing dolomitization and the disappearance of reef corals towards the top of the Maniyara Formation, documents a decreasing accommodation space due to the advancing uplift of the KMU tilt block (Fig. 3). As a result of this tectonic movement extensive parts of the KMU became permanently exposed in higher elevated areas at the onset of the Aquitanian and the Oligocene and Eocene cover was removed. This unroofed the about 3000-m-thick siliciclastic Mesozoic core of the KMU and its siliciclastic weathering products suffocated the carbonate ramp. Since that time the shallow-marine carbonate factory was not able to recover in the Kachchh Basin due to a steady input of siliciclastic sediments.

5.4 Origin of event deposits: tempestite versus tsunamite

At the recent coast of Kachchh high-energy wave events which are capable of eroding sediments in relatively deep water and redepositing these in shallow water are caused by tsunamis and tropical cyclones (Nigam and Chaturvedi, 2006). Both processes

CPD
9, 583–613, 2013

result in a mixing of skeletal components representing different environments and can form vast shell beds (Kortekaas and Dawson, 2007; Donato et al., 2008). Synsedimentary uplift of the KMU block indicates that tsunamis may have been triggered by seismic activity at the northwestern margin of India, which was related to transpressional tectonics in response to the convergent movement of Asia and India during the Late Oligocene (Shanker, 2001; Gunnell et al., 2003; Sheth, 2007). Since most of the research on tsunami deposits focuses on onshore areas and siliciclastic coasts and most established criteria also apply for storm deposits (e.g. Fujiwara and Kamataki, 2007; Morton et al., 2007; Donato et al., 2008; Feldens et al., 2009; Bahlburg et al., 2010; Engel and Brückner, 2011), the identification of tsunamites in particular in shallow-marine carbonate environments remains extremely difficult. The shell beds of the Maniyara Formation formed exclusively in a shallow inner ramp setting on the gentle inclined homoclinal KMU ramp. This setting is most intensely affected by erosion of an incoming tsunami wave (Puga-Bernabéu et al., 2007). The subsequent backflow transports the previously eroded sediments basinwards and produces a thick shell-debris bed on the deeper ramp (Puga-Bernabéu et al., 2007), while near-shore backflow sediments have a patchy or channelized distribution (scour-and-fill structures; Einsele et al., 1996; Feldens et al., 2009). Since these features are missing tsunami-events cannot account for the extensive shell beds of the Maniyara Fort Formation.

In contrast, coarse-grained (proximal) tempestites can cover extensive areas on shallow ramparts (Seilacher and Aigner, 1991; Rasser and Riegl, 2002; Flügel, 2004). The uppermost larger foraminiferan shell bed in the Coral Limestone Member differs from all other shell beds by its wedge-shaped geometry and muddy glauconitic matrix (Fig. 2). A modern analogue may represent the coastal mud wedges, which were produced by Hurricane Andrew at the southwest Florida coast (Risi et al., 1995). These up to 1 m thick and over 3 km long sediment wedges formed just seaward of the shoreline as the surge flood water retreated. Consistently with this interpretation, the wedge-shaped shell bed in the Coral Limestone Member formed at the onset of flooding after a sea level lowstand (Fig. 3) and the fine-grained terrigenous matrix indicates strong

CPD
9, 583–613, 2013

sediment discharge from a closeby hinterland. In contrast, the pure carbonatic sheet-like shell concentrations possibly formed when the shallow carbonate ramp was isolated from a hinterland during the inundation episodes (Fig. 3). At present-day, tropical cyclones develop only in regions where the sea surface temperature is above 26.5 °C and where the depth of the 26 °C isotherm is 60 m or more (Gray, 1998). Most of them occur between 20° N and 20° S and no formations occur within about 2.5° latitude of the equator (Gray, 1968). The Late Oligocene Kachchh Basin was located at 11° N (Chatterjee et al., 2012) in the tropical cyclone belt and the studied tempestite sequence corresponds to the Late Oligocene warming period (∼ 27–24 Ma) when the long-term glaciation of Antarctica terminated (Zachos et al., 2001, 2008; von der Heydt and Dijkstra, 2006).

5.5 Tropical cyclone variability during Late Oligocene sea level highstands

The low palaeodepth gradients during the inundation episodes (Fig. 3) show that changing compositions of the skeletal assemblages in the tempestites of the Maniyara Fort Formation must reflect a shifting of the storm wave base rather than water depth fluctuations related to sea level changes (Fig. 4). A shallow storm wave base is shown by the association of nearshore mollusc faunas with abundant *Clypeaster* echinoids and reef corals (Fig. 4c). An intermediate depth of the storm wave base is indicated by mass accumulations of lepidocyclinids with frequent *Eupatagus* echinoids and/or some amounts of corallinaceans (Fig. 4b) and the deepest storm wave base is represented by the *Amussiopecten–Schizaster* assemblage (Fig. 4a).

Eustatic sea level and climate are closely linked: as the climate warms the sea level rises due to the melting of the global ice sheets and as the seas warm the ocean has more energy to generate tropical cyclone winds (Elsner et al., 2008). Accordingly for the third-order sea level highstand that follows on the Ch3 sequence boundary of Hardenbol et al. (1998) the stratigraphic distribution of the defined tempestite skeletal assemblage types show the deepest storm wave base at maximum flooding during the insolation maximum (Dutton et al., 2009) (Figs. 2, 3). The gradual shifts in the

CPD
9, 583–613, 2013

composition of the tempestite skeletal assemblages (Fig. 2) reflect continuous deepening/shallowing of the storm wave base during the early and late highstand. In contrast, weak storm intensity is indicated for the highstand of the previous third-order sea level cycle by the absence of tempestites during maximum flooding (Fig. 2).

5.6 Monsoon impact on Late Oligocene tropical cyclone trends

An important pre-condition for cyclone formation is a large-scale environment with small vertical wind shear (Gray, 1968). In the recent Arabian Sea the average sea surface temperatures are warm enough to support the development of tropical cyclones throughout the year but the Indian summer monsoon (SW-monsoon) and associated vertical shear wind limit cyclone development and intensification (Evan et al., 2011). The strength of the vertical wind shear is dependent on the strength of the Indian summer monsoon and the associated tropical easterly jet higher up in the atmosphere. The high-altitude winds flow from the opposite direction of the low-level monsoon winds creating a high vertical wind shear over the Arabian Sea, which halts cyclone formation by blowing off the tops of tropical storms (Hubert et al., 1983; Rao et al., 2008; Krishna, 2009). Weakening of the Indian summer monsoon is favorable for the formation of more severe tropical storms over the Arabian Sea because it is coupled to a decrease of the vertical wind shear (Rao et al., 2008; Evan et al., 2011).

The Indian monsoon is an integral part of the Asian monsoon system. Of greatest relevance to the strength of this large-scale atmospheric circulation is the land–sea thermal contrast that creates a vast low-pressure system over Central Asia during summer drawing in warm and humid air from the Arabian Sea towards the Tibetan Plateau (Webster et al., 1998). Due to this thermal and further orographic controls Himalayan–Tibetan Plateau uplift since the Indo–Asia collision has been inferred to be the main force for the evolution of the Asian monsoon (e.g. Ruddiman and Kutzbach, 1989; Raymo and Ruddiman, 1992). Uplift of this area began about 50 Ma (Eocene) during the initial collision and was intensified during the Early Miocene (Chatterjee et al., 2012). The onset of aeolian deposition on the Chinese Loess Plateau shows that

Discussion Paper | Discussion Paper | Discussion Paper | Discussion Paper |

CPD

9, 583–613, 2013

Cyclone trends constrain monsoon variability

M. Reuter et al.

the major change towards an Asian monsoon climate was achieved at ~22 Ma (Early Miocene; Guo et al., 2002, 2008) (Fig. 5). Since then the overall trend is one of gradually increasing monsoon strength to 10 Ma (Late Miocene) with an unusually weak monsoon at 16.5 to 15 Ma (Clift et al., 2008). The exact timing of Tibetan Plateau uplift is, however, a matter of considerable debate (Wang et al., 2008) and there is some emerging evidence for regionally high Tibetan palaeoelevations early on in the Indo-Asia collision indicating that an early plateau formation may have already contributed to monsoon intensification at the Eocene/Oligocene transition (Dupont-Niovet et al., 2008; Hoorn et al., 2012: further references therein).

In line with these evidences, and since the winds over the Arabian Sea are considered as meaningful indicators for the strength of the Indian monsoon (Wang et al., 2003), the reconstructed Late Oligocene storm trends in the Kachchh Basin may reflect monsoon variability during the early stages of the Asian monsoon system. For the late highstand of the first Chattian third-order sea level cycle, the larger benthic foraminiferan tempestite sequence at the base of the Maniyara Fort Formation indicates frequent storms with moderately deep wave base due to an absent or weak Indian monsoon. In contrast, the absence of tempestites during the acme of the second Chattian third-order sea level cycle suggests that a strong Indian monsoon prevented tropical cyclogenesis at ~26 Ma. Subsequent weakening of the Indian monsoon is indicated by renewed tempestite sedimentation during the late highstand of this sea level cycle. However the absence of deep water indicators and the low abundance and small size of larger benthic foraminifers indicate at first relatively weak storms with shallow wave base. Prolonged weakening of the Indian monsoon may have subsequently favored violent tropical storms with deep wave base, which produced the *Amussiopecten*- and *Schizaster*-dominated tempestites during the next third-order sea level highstand that follows the Ch3 sequence boundary of Hardenbol et al. (1998). Interestingly, this storm interval correlates to the temperature maximum of the Late Oligocene warm period (Zachos et al., 2008) (Fig. 5).

A comparable Asian monsoon decline over northern India and China has been recorded at 16.5–15 Ma in weathering records from the Arabian Sea, the Bay of Bengal and the South China Sea (Clift et al., 2008; Wan et al., 2010). It corresponds to the Middle Miocene Climate Optimum (Fig. 5), when the global annual surface temperature was ~3–4° C higher than today (You, 2010) and the thermal gradient between the Tibetan Plateau and tropical Indian Ocean was reduced (Reuter et al., 2012). An analogous scenario can be reconstructed for the temperature maximum of the Late Oligocene warming due to a similar land–sea configuration (PALEOMAP website) and a comparable $\delta^{18}O$ range in the deep sea oxygen isotope record (Zachos et al., 2008) (Fig. 5). The heavier $\delta^{18}O$ values during the third-order sea level highstand at ~26 Ma in the deep sea oxygen isotope record of Zachos et al. (2008) (Fig. 5) suggest that this temperature rise was not high enough to prevent the Indian monsoon and favor cyclogenesis off the northwestern coast of India.

6 Conclusions

The Maniyara Fort Formation (Upper Oligocene) in the Kachcch Basin (NW India) comprises a succession of vast shell beds composed of larger benthic foraminifers, molluscs and echinoids that were deposited in an isolated inner ramp environment. The sedimentation occurred only during third-order sea level highstands separated by long lasting erosional gaps. The skeletal components represent a mixture of different marine environments documenting extensive sediment transport from deep to shallow water by severe tropical storms (cyclones). Three major biotic assemblages point to variable storm intensities: (1) shallow storm reworking is indicated by nearshore gastropods, *Clypeaster* echinoids and reef corals; (2) an intermediated storm wave base is reflected in larger benthic foraminiferan (lepidocyclinids) deposits with abundant *Eupatagus* echinoids and corallinaceans; (3) a deep storm wave base caused high amounts of *Amussiopecten* and *Schizaster* echinoids in the tempestites. Vertical changes in these skeletal associations give evidence of a deepening storm wave depth

CPD
9, 583–613, 2013

due to increasing tropical storm intensities during a third-order sea level rise. The intensity of tropical cyclones is controlled over the recent Arabian Sea by the strength of the vertical wind shear, which is depending on the strength of the Indian summer monsoon. Accordingly the reconstructed longer-term storm trends from the Maniyara Fort Formation are interpreted to reflect monsoon variability over northern India during the Late Oligocene. For the third-order sea level highstand that follows on the Ch2 sequence boundary (∼ 26 Ma) the low tempestite frequency and relative shallow storm wave base depth suggest already the action of a relative strong Indian monsoon. In contrast, a weak Indian monsoon is indicated for the next third-order sea level highstand (∼ 24 Ma) by frequent tempestites representing a deep storm wave base. This Indian monsoon decline correlates to the temperature maximum of the Late Oligocene warming and implies that this global temperature rise had largely reduced the land–sea thermal contrast between the Tibetan Plateau and the tropical Eastern Tethys.

Acknowledgements. We are indebted to D. Banerjee (Delhi) for organizing the local contacts and the Bhatti family (Bhuj) for their great hospitality and logistic support. Sanghi Cement is thanked for free lodging and catering B. Berning (Linz) attended field work, D. Bassi (Ferrara) kindly identified the larger benthic foraminifers and M. Gross (Graz) determined the ostracods. T. Wagner (Graz) created the digital elevation model. Funding by the FWF (Fonds zur Förderung der wissenschaftlichen Forschung) through grants P23492 and P18189 is gratefully acknowledged.

References

Ali, J. R. and Aitchison, J. C.: Gondwana to Asia: Plate tectonics, paleogeography and the biological connectivity of the Indian sub-continent from the Middle Jurassic through latest Eocene (166–35 Ma), Earth Sci. Rev., 88, 145–166, 2008.

Bahlburg, H., Spiske, M., and Weiss, R.: Comment on “Sedimentary features of tsunami backwash deposits in a shallow marine Miocene setting, Mejillones Peninsula, northern Chile”, Sediment. Geol., 228, 77–80, 2010.

Bandel, K. and Wedler, E.: Hydroid, amphineuran and gastropod zonation in the littoral of the Caribbean Sea, Colombia, Senckenbergiana maritima, 19, 1–129, 1987.
Bassi, D., Hottinger, L., and Nebelsick, J. H.: Larger foraminifera from the Upper Oligocene of the Venetian area, North-East Italy, Palaeontology, 50, 845–868, 2007.
Biswas, S. K.: Rift basins in the western margin of India and their hydrocarbon prospects Bull. Am. Assoc. Petrol. Geol., 66, 1497–1513, 1982.
Biswas, S. K.: Regional tectonic framework, structure and evolution of the western marginal basins of India, Tectonophysics, 135, 307–327, 1987.
Biswas, S. K.: Tertiary stratigraphy of Kutch, J. Palaeontol. Soc. India, 37, 1–29, 1992.
Biswas, S. K.: A review of structure and tectonics of Kutch Basin, western India, with special reference to earthquakes, Curr. Sci., 88, 1592–1600, 2005.
Biswas, S. K. and Deshpande, S. V.: Mode of eruption of Deccan Trap lavas with special reference to Kutch, J. Geol. Soc. India, 14, 134–141, 1973.
Biswas, S. K. and Raju, D. S. N.: Note on rock-stratigraphic classification on the Tertiary sediments of Kutch, Q. J. Geol. Min. Metall. Soc. India, 43, 177–180, 1971.
Brand, A. R.: 2006 Scallop ecology: distributions and behaviour, in: Scallops: Biology, Ecology and Aquaculture, G. J., Dev. Aquaculture Fish. Sci., 35, 651–744, 2006.
Brandt, D. S. and Elias, R. J.: Temporal variations in tempestite thickness may be a geological record of atmospheric CO_2, Geology, 17, 951–952, 1989.
Brett, C. E. and Seilacher, A.: Fossil Lagerstätten: a taphonomic consequence of event sedimentation in: Cycles and Events in Stratigraphy, edited by: Einsele, G., Ricken, W., and Seilacher, A., Springer-Verlag, Berlin, Heidelberg, 283–297, 1991.
Cahuzac, B. and Poignant, A.: Essai de biozonation de l'Oligo-Miocène dans les basins européens à l'aide des grands foraminifères nèritiques, Bull. Soc. Géol Fr., 168, 155–169, 1997.
Charabi, Y: Preface, in: Indian Ocean Tropical Cyclones and Climate Change, edited by: Charabi, Y., Springer, Dordrecht, 2010.
Chatterjee, S., Goswami, A., and Scotese, C. R.: The longest voyage: Tectonic, magmatic, and paleoclimatic evolution of the Indian plate during its northward flight from Gondwana to Asia, Gondwana Res., 23, 238–267, 2012.
Clift, P. D., Hodges, K. V.,Heslop, D., Hannigan, R., van Long, H., and Calves, G.: Correlation of Himalayan exhumation rates and Asian monsoon intensity, Nat. Geosci., 1, 875–880, 2008.

de Ridder, C.: Clypeastéroïdes et spatangoïdes littoraux de Nouvelle-Calédonie (Echinodermata), Bull Mus. Natl. Hist. Nat. A, 6, 617–624, 1984.
Donato, S. V., Reinhardt, E. G., Boyce, J. I., Rothaus, R., and Vosmer, T.: Identifying tsunami deposits using bivalve shell taphonomy, Geology, 36, 199–202, 2008.
Dupont-Nivet, G., Hoorn, C., and Konert, M.: Tibetan uplift prior to the Eocene-Oligocene climate transition: Evidence from pollen analysis of the Xining Basin, Geology, 36, 987–990, 2008.
Dutton, A., Antonioli, F., and Bard, E.: A new chronology of sea level highstands for the penultimate interglacial, Pages News, 17, 66–68, 2009.
El Albani, A., Meunier, A., and Fürsich, F.: Unusual occurrence of glauconite in a shallow lagoonal environment, Terra Nova, 17, 537–544, 2005.
Elsner, J. B., Kossin, J. P., and Jagger, T. H.: The increasing intensity of the strongest tropical cyclones, Nature, 455, 92–95, 2008.
Einsele, G., Chough, S. K, and Shiki, T.: Depositional events and their records – an introduction Sediment Geol., 104, 1–9, 1996.
Engel, M. and Bückner, H.: The identification of palaeo-tsunami deposits – a major challenge in coastal sedimentary research, Coastline Reports, 17, 65–80, 2011.
Emanuel, K. A., Sundarajan, R., and Williams, J.: Hurricanes and global warming: Results from downscaling IPCC AR4 simulations, B. Am. Meteorol. Soc., 89, 347–367, 2008.
Evan, A. T., Kossin, J. P., Chung, C., and Ramanathan, V.: Arabian Sea tropical cyclones intensified by emissions of black carbon and other aerosols, Nature, 479, 94–97, 2011.
Feldens, P., Schwarzer, K., Szczuciński, W., Stattegger, K., Sakuna, D., and Somgpongchaiykul, P.: Impact of 2004 tsunami on seafloor morphology and offshore sediments, Pakarang Cape, Thailand, Pol. J. Environ. Stud., 18, 63–68, 2009.
Flügel, E.: Microfacies of Carbonate Rocks: Analysis, Interpretation and Application Springer-Verlag, Berlin, Heidelberg, 2004.
Fujiwara, O. and Kamataki, T.: Identification of tsunami deposits considering the tsunami waveform: An example of subaqueous tsunami deposits in Holocene shallow bay on southern Boso Peninsula, Central Japan, Sediment Geol., 200, 295–313, 2007.
Goldenberg, S. B., Landsea, C., Mestas-Nunez, A. M., and Gray, W. M.: The recent increase in Atlantic hurricane activity, Science, 293, 474–479, 2001.
Gradstein, F. M., Ogg, J. G., Schmitz, M. D., and Ogg, G. M.: The Geologic Time Scale 2012, Elsevier, Amsterdam, 2012.

Gray, W. M.: Global view of the origin of tropical disturbances and storms, Mon. Weather Rev., 96, 669–700, 1968.
Gray, W. M.: The formation of tropical cyclones, Meteorol. Atmos Phys., 67, 37–69, 1998.
Gunnell, Y., Gallagher, K., Carter, A., Widdowson, M., and Hurford, A. J.: Denudation history of the continental margin of western peninsular India since the early Mesozoioc – reconciling apatite fission-track data with geomorphology, Earth Planet Sc. Lett., 215, 187–201, 2003.
Guo, Z. T., Ruddiman, W. F., Hao, Q. Z., Wu, H. B., Qiao, Y. S., Zhu, R. X., Peng, S. Z., Wei, J. J., Yuan, B. Y., and Liu, T. S.: Onset of Asian desertification by 22 Myr ago inferred from loess deposits in China, Nature, 416, 159–163, 2002.
Guo, Z. T., Sun, B., Zhang, Z. S., Peng, S. Z., Xiao, G. Q., Ge, J. Y., Hao, Q. Z., Qiao, Y. S., Liang, M. Y., Liu, J. F., Yin, Q. Z., and Wei, J. J.: A major reorganization of Asian climate by the early Miocene, Clim. Past, 4, 153–174, doi:10.5194/cp-4-153-2008, 2008.
Hardenbol, J., Thierry, J., Farley, M. B., Jacquin, T., Graciansky, P.-C., and Vail, P. R.: Mesozoic and Cenozoic sequence chronostratigraphic framework of European basins, in: Mesozoic and Cenozoic Sequence Stratigraphy of European Basins, edited by: Graciansky, C.-P., Hardenbol, J., Jacquin, T., and Vail, P. R., SEPM Special Publications, 60, 3–13, 1998.
Harzhauser, M., Reuter, M., Piller, W. E., Berning, B., Kroh, A., and Mandic, O.: Oligocene and Early Miocene gastropods from Kutch (NW-India) document an early biogeographic switch from Western Tethys to Indo-Pacific, Paläont. Z., 83, 333–372, 2009.
Henderson-Sellers, A., Zhang, H., Berz, G., Emanuel, K., Gray, W., Landsea, C., Holland, G., Lighthill, J., Shieh, S.-L., Webster, P., and McGuffie, K.: Tropical cyclones and global climate change: a post-IPCC assessment, B. Am. Meteorol. Soc., 79, 19–38, 1998.
Hendler, G., Miller, J. E., Pawson, D. E., and Kier, P. M.: Echinoderms of Florida and the Carribean, Smithsonian Institution Press, Washington, 1995.
Himmelman, J. H., Guderley, H. E., and Duncan, P. F.: Responses of the saucer scallop *Amusium balloti* to potential predators, J. Exp. Mar. Biol. Ecol., 378, 58–61, 2009.
Holland, G. J. and Webster, P. J.: Heigthened tropical cyclone acivity in the North Atlantic: Natural variability or climate trend?, Phil. Trans. R. Soc. A, 365, 2695–2716, 2007.
Hoorn, C., Straathof, J., Abels, H. A., Xu, Y., and Utescher, T.: A late Eocene palynological record of climate change and Tibetan Plateau uplift (Xining Basin, China), Palaeogeogr. Palaeocl., 344–345, 16–38, 2012.

Hubert, W. E., Hull, A. N., Morford, D. R., and Englebretson, R. E.: Forecasters Handbook for the Middle East/Arabian Sea. United States Navy, Naval Environmental Prediction Research Facility, Monterey, California, available at: http://www.nrlmry.navy.mil/forecaster_handbooks/EastArabianSea/Forecasters%20Handbook%20for%20the%20Middle%20East-Arabian%20Sea.htm (last acess: 18 January 2013), 1983.
Jarvis, A., Reuter, H. I., Nelson, E., and Guevara, E.: Hole-filled SRMT for the globe Version 4. CGIAR-CSI SRTM 90 m Database, available at: http://srtm.csi.cgiar.org/ (last acess: 18 January 2013), 2008.
Kanazawa, K.: Adaptation of test shape for burrowing and locomotion in spatangoid echinoids, Palaeontology, 35, 733–750, 1992.
Klotzbach, P. J.: Trends in global tropical cyclone activity over the past twenty years (1986–2005), Geophys. Res. Lett., 33, L10805, doi:10.1029/2006GL025881, 2006.
Knutson, T. R., McBride, J. L., Chan, J., Emanuel, K., Holland, G., Landsea, C., Held, I., Kossin, J. P., Srivastava, A. K., and Sugi, M.: Tropical cyclones and climate change, Nat. Geosci., 3, 157–163, 2010.
Kornicker, L. S.: Ecology and taxonomy of Recent Bairdiinae (Ostracoda), Micropaleontology 7, 55–70, 1961.
Kortekaas, S. and Dawson, A. G.: Distinguishing tsunami and storm deposits: an example from Martinhal, SW Portugal, Sediment Geol., 200, 208–221, 2007.
Krishna, K. M.: Intensifying tropical cyclones over the North Indian Ocean during summer monsoon – global warming, Global Planet. Change, 65, 12–16, 2009.
Long, D. G. F.: Tempestite frequency curves: a key to Late Ordovician and Early Silurian subsidence, sea-level change, and orbital forcing in the Anticosti foreland basin, Quebec, Canada, Can. J. Earth Sci., 44, 413–431, 2007.
Mandic, O. and Piller, W. E.: Pectinid coquinas and their palaeoenvironmental implications – examples from the early Miocene of northeastern Egypt, Palaeogeogr. Palaeocl., 172, 171–191, 2001.
Mortensen, T.: A Monograph of the Echinoidea, V, 2. Spatangoida I I. Amphisternata I I. Spatangidæ, Loveniidæ, Pericosmidæ, Schizasteridæ, Brissidae, C. A. Reitzel, Copenhagen, 1951.
Morton, R. A., Gelfenbaum, G., and Jaffe, B. E.: Physical criteria for distinguishing sandy tsunami and storm deposits using modern examples, Sediment. Geol., 200, 184–207, 2007.

Nigam, R. and Chaturvedi, S. K.: Do inverted depositional sequences and allochthonous foraminifers in sediments along the Coast of Kachchh, NW India, indicate palaeostorm and/or tsunami effects?, Geo-Mar. Lett., 26, 42–50, 2006.
PALEOMAP website: available at: http://www.scotese.com/, last access: 12 December 2012.
Pedley, M.: A review of sediment distributions and processes in Oligo-Miocene ramps of southern Italy and Malta (Mediterranean divide), in: Carbonate Ramps, edited by: Wright, V. P. and Burchette, T. P., Geol. Soc. London Spec. Publ., 149, 163–179, 1998.
Puga-Bernabéu, Á., Martín, J. M., and Braga, J. C.: Tsunami-related deposits in temperate carbonate ramps, Sorbas Basin, southern Spain, Sediment. Geol., 199, 107–127, 2007.
Quan, C., Liu, Y. S., and Utescher, T.: Paleogene evolution of precipitation in northeastern China supporting the middle Eocene intensification of the East Asian monsoon, Palaios, 26, 743–753, 2011.
Rao, V. B., Ferreira, C. C., Franchito, S. H. and Ramakrishna, S. S. V. S.: In a changing climate weakening tropical easterly jet induces more violent tropical storms over the north Indian Ocean, Geophys. Res. Lett., 35, L15710, doi:10.1029/2008GL034729, 2008.
Rasser, M. W. and Riegl, B.: Holocene coral reef rubble and its binding agents, Coral Reefs, 21, 57–72, 2002.
Raymo, M. E. and Ruddiman, W. F.: Tectonic forcing of late Cenozoic climate, Nature, 359, 117–122, 1992.
Reuter, M., Piller, W. E., Harzhauser, M., Kroh, A., and Bassi, D.: Termination of the Arabian shelf sea: stacked cyclic sedimentary patterns and timing (Oligocene/Miocene, Oman), Sediment. Geol., 212, 12–24, 2008.
Reuter, M., Kern, A. K., Harzhauser, M., Kroh, A., and Piller, W. E.: Global warming and South Indian monsoon rainfall–lessons from the Mid-Miocene, Gondwana Res., online first, doi:10.1016/j.gr.2012.07.015, 2012.
Risi, A., Wanless, H. R., Tedesco, L. P., and Gelsanliter, S.: Catastrophic sedimentation from Hurricane Andrew along the Southwest Florida Coast, J. Coast. Res., 21, 83–102, 1995.
Ruddiman, W. F. and Kutzbach, J. E.: Forcing of late Cenozoic Northern Hemisphere climate by plateau uplift in southern Asia and American west, J. Geophys. Res., 94, 409–427, 1989.
Saunders, A. D., Jones, S. M., Morgan, L. A., Pierce, K. L., Widdowson, M., and Xu, Y. G.: Regional uplift associated with continental large igneous provinces: the role of mantle plumes and the lithosphere, Chem. Geol., 241, 282–318, 2007.

CPD
9, 583–613, 2013

Cyclone trends constrain monsoon variability

M. Reuter et al.

Schinner, G. O.: Burrowing behaviour, substratum preference, and distribution of *Schizaster canaliferus* (Echinoidea: Spatangoida) in the Northern Adriatic Sea, Mar. Ecol., 14, 129–145, 1993.
Schultz, H.: Sea Urchins: a guide to worldwide shallow water species, Heinke & Peter Schultz Partner, Hemdingen, 2005.
Schultz, H.: Sea Urchins II: worldwide irregular deep water species, Heinke & Peter Schultz Partner, Hemdingen, 2009.
Seilacher, A. and Aigner, T.: Storm deposition at the bed, facies, and basin scale: the geological perspective, in: Cycles and Events in Stratigraphy, edited by: Einsele, G., Ricken, W., and Seilacher, A., Springer-Verlag, Berlin, Heidelberg, 249–267, 1991.
Sepkowski Jr., J. J., Bambach, R. K., and Droser, M. L.: Secular changes in Phanerozoic event bedding and biological overprint, in: Cycles and Events in Stratigraphy, edited by: Einsele, G., Ricken, W., and Seilacher, A., Springer-Verlag, Berlin, Heidelberg, 298–312, 1991.
Shanker, R.: Seismotectonics of Kutch rift basin and its bearing on the Himalayan seismicity, ISET Journal of Earthquake Technology, 38, 59–65, 2001.
Sheth, H. C.: Plume-related regional pre-volcanic uplift in the Deccan Traps: Absence of evidence, evidence of absence in: Plates, Plumes and Planetary Processes, edited by: Foulger, G. R. and Jurdy, D. M., Geol. Soc. Am. Spec. Pap., 430, 785–813, 2007.
Solomon, S., Qin, D., Manning, M., Chen, Z., Marquis, M., Averyt, K. B., Tignor, M., and Miller, L.: Contribution of Working Group I to the Fourth Assessment Report of the Intergovernmental Panel on Climate Change, Cambridge University Press, Cambridge, 2007.
Valeton, I.: Saprolite-bauxite facies of ferralitic duricrusts on palaeosurfaces of former Pangaea, in: Palaeoweathering, Palaeosurfaces, and Related Continental Deposits, edited by: Thiry, M. and Simon-Coinçon, R., IAS Spec. Publ., 27, 153–188, 1999.
Vecchi, G. A. and Knutson, T. R.: On estimates on historical North Atlantic tropical cyclone activity, J. Climate 21, 3580–3600, 2008.
von der Heydt, A. and Dijkstra, H. A.: Effect of ocean gateways on the global ocean circulation in the late Oligocene and early Miocene, Paleoceanography, 21, PA1011, doi:10.1029/2005PA001149, 2006.
Wan, S., Clift, P. D., Li, A., Li, T., and Yin, X.: Geochemical records in the South China Sea: implications for East Asian summer monsoon evolution over the last 20 Ma in: Monsoon Evolution and Tectonics – Climate linkage in Asia, edited by: Clift, P. D., Tada, R., and Zheng, H., Geol. Soc. London Spec. Publ., 342, 245–263, 2010.

CPD
9, 583–613, 2013

Wang, B., Clemens, S. C., and Liu, P.: Contrasting the Indian and East Asian monsoons: implications on geological timescales, Mar. Geol., 201, 5–21, 2003.
Wang, Y., Wang, X., Xu, Y., Zhang, C., Li, Q., Tseng, Z. J., Takeuchi, G., and Deng, T.: Stable isotopes in fossil mammals, fish and shells from Kunlun Pass Basin, Tibetan Plateau: Paleo-climatic and paleo-elevation implications, Earth Planet. Sc. Lett., 270, 73–85, 2008.
Wanless, H. R., Tedesco, L. P., and Tyrell, K. M.: Production of subtidal tubular and surficial tempestites by Hurricane Kate, Caicos Platform, British West Indies, J. Sediment. Petrol., 58, 739–750, 1988.
Webster, P. J., Magana, V. O., Palmer, T. N., Shukla, J., Tomas, R. A., Yanai, M., and Yasunari, T.: Monsoons: processes, predictability, and the prospects for prediction, in the TOGA decade, J. Geophys. Res., 103, 14451–14510, 1998.
Webster, P. J., Holland, G. J., Curry, J. A., and Chang, H.-R.: Changes in tropical cyclone number, duration and intensity in a warming environment, Science, 309, 1844–1846, 2005.
You, Y.: Climate-model evaluation of the contribution of sea-surface temperature and carbon dioxide to the Middle Miocene Climate Optimum as a possible analogue of future climate change, Aust. J. Earth Sci., 57, 207–219, 2010.
Zachos, J., Pagani, M., Sloan, L., Thomas, E., and Billups, K.: Trends, rhythms, and aberrations in global climate 65 Ma to present, Science, 292, 686–693, 2001.
Zachos, J. C., Dickens, G. R., and Zeebe, R. E.: An early Cenozoic perspective on greenhouse warming and carbon-cycle dynamics, Nature, 451, 279–283, 2008.

CPD
9, 583–613, 2013

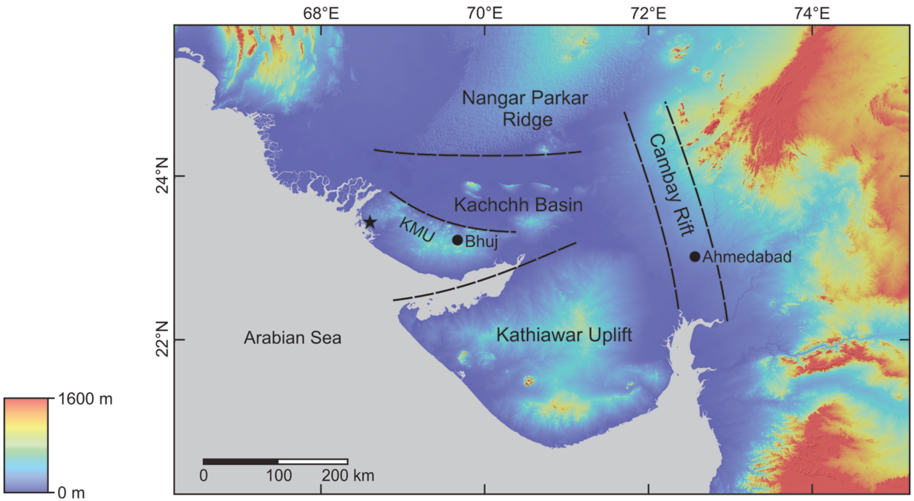

Fig. 1. Digital elevation model of northwestern India (Jarvis et al., 2008) showing the main structural geological elements of the Kachchh Basin. The black asterisk locates the studied outcrop at Bermoti (23°27′45″ N, 68°36′07″ E) on the Kachchh Mainland Uplift (KMU).

CPD
9, 583–613, 2013

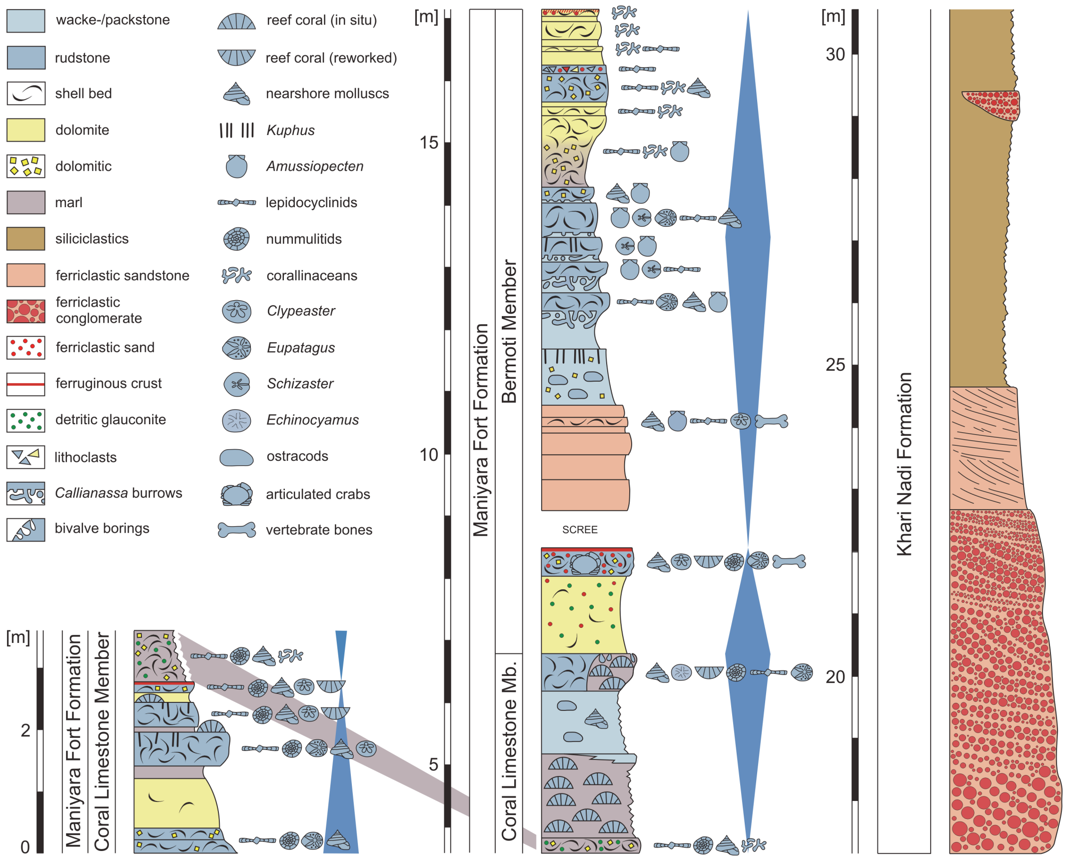

Fig. 2. Bermoti river section. Lithological log, lithostratigraphy (Biswas, 1992) and depositional sequences.

CPD
9, 583–613, 2013

Cyclone trends constrain monsoon variability

M. Reuter et al.

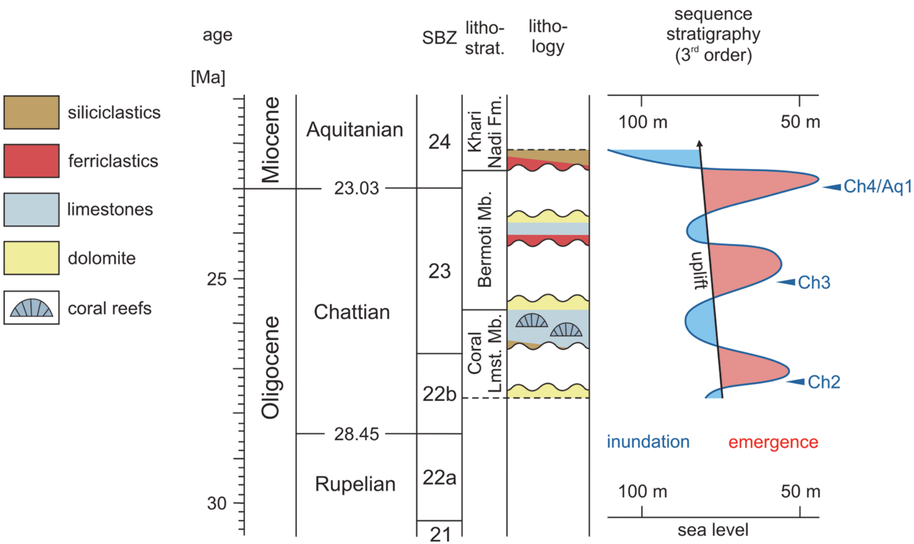

Fig. 3. Stratigraphic correlation of Bermoti river section with the shallow benthic foraminifera zones (SBZ) of Cahuzac and Poignant (1997), third-order sequences of Hardenbol et al. (1998) and global chronostratigraphy (Gradstein et al., 2012). Lithostratigraphy according to Biswas (1992).

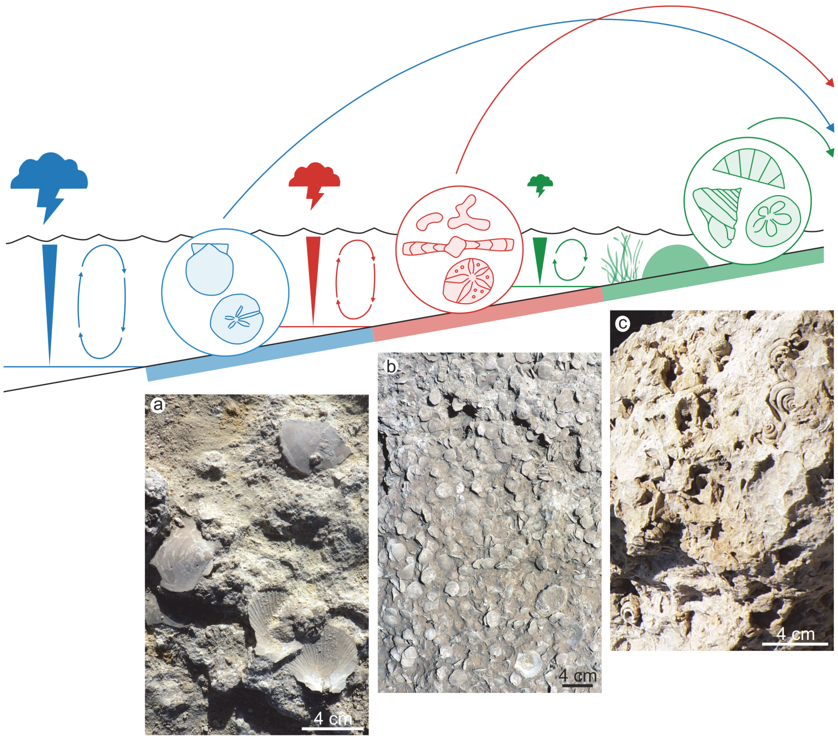

Fig. 4. Facies model for shallow-marine tempestite deposition on the Kachcch Mainland Uplift carbonate ramp illustrating the relationships of skeletal composition and storm intensity (cloud symbol: green = weak, red = moderate, blue = strong). The thick vertical arrowheads indicate the storm wave base depth; the symbols representing the defined tempestite biotic assemblages refer to Fig. 2. **(a)** Tempestites with abundant *Amussiopecten* represent the deepest storm wave base. **(b)** A moderately deep storm wave base is indicated by reworking and nearshore deposition of large lepidocyclinids. **(c)** Gastropod shell beds document storm reworking in shallow water.

CPD
9, 583–613, 2013

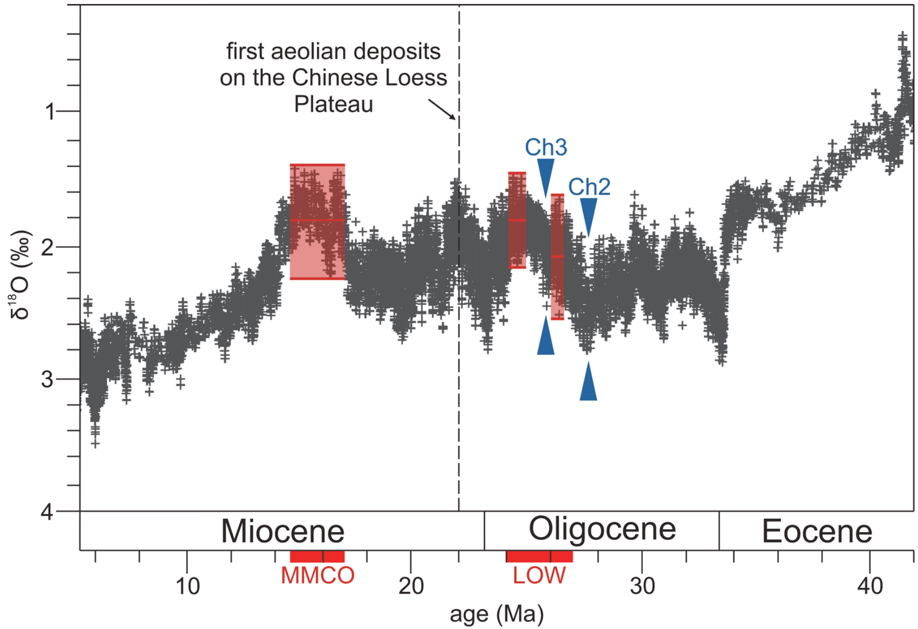

Fig. 5. Deep sea benthic foraminiferal oxygen isotope curve as estimate for the Eocene–Miocene evolution of the global climate (modified after Zachos et al., 2008; LOW = Late Oligocene Warming, MMCO = Middle Miocene Climate Optimum). Blue arrowheads indicate the Ch2 and Ch3 sequence boundaries of Hardenbol et al. (1998). The onset of aeolian sedimentation on the Chinese Loess Plateau is considered as proxy for the initiation of the Asian monsoon (Guo et al., 2002).

CPD
9, 583–613, 2013